

# Size- and Shape-Dependent Polarizabilities of Sandwich and Rice-Ball $\text{Co}_n\text{Bz}_m$ Clusters from Density Functional Theory

Jinlan Wang,<sup>\*,†</sup> Liyan Zhu,<sup>†</sup> Xiuyun Zhang,<sup>†</sup> and Mingli Yang<sup>\*,‡</sup>

Department of Physics, Southeast University, Nanjing 211189, China, and Institute for Nanobiomedical Technology, State Key Laboratory of Biotherapy, West-China Medical School/West-China Hospital, Sichuan University, Chengdu 610041, China

Received: April 14, 2008; Revised Manuscript Received: May 25, 2008

The dipole polarizabilities of  $\text{Co}_n\text{Bz}_m$ , ( $n, m = 1-4, m = n, n + 1$ ) clusters are studied by means of an all-electron gradient-corrected density functional theory and finite field method. The dipole moments are relatively large for most of the clusters, implying their asymmetric structures. The total polarizability increases rapidly as cluster size, whereas the average polarizability shows “odd–even” oscillation with relatively large values at ( $n, n + 1$ ). The polarizabilities exhibit clear shape-dependent variation, and the sandwich structures have systematically larger polarizability and anisotropy than the rice-ball isomers. The dipole polarizabilities are further analyzed in terms of the highest occupied molecular orbital–lowest unoccupied molecular orbital (HOMO–LUMO) gap, ionization potential, and electron delocalization volume. We conclude that the polarizability variations are determined by the interplay between the geometrical and electronic properties of the clusters.

## I. Introduction

Metal–ligand complexes comprised of transition metal (TM) atoms and benzene molecules ( $\text{TM}_n\text{Bz}_m$ ,  $\text{Bz} = \text{C}_6\text{H}_6$ ) have attracted enormous interest either from a fundamental science or application point of view in the past decades.<sup>1,2</sup> Earlier ion mobility, reactivity, and photoelectronic spectroscopic experiments suggested that multidecked sandwich structures are favored for early transition metal (Sc, Ti, V) complexes and rice-ball conformations for late ones (Fe, Co, Ni).<sup>3–5</sup> More interestingly, both Stern–Gerlach molecular beam deflection experiments and density functional theory (DFT) computations revealed the complexes like  $\text{V}_n\text{Bz}_{n+1}$  and  $\text{Co}_n\text{Bz}_m$  are magnetic, whereas  $\text{Ti}_n\text{Bz}_{n+1}$  are paramagnetic.<sup>6–13</sup>

The experimental and theoretical explorations on optical properties of TM–Bz complexes have also been made although most studies are restricted to small sizes like half-sandwich and smallest full sandwich.<sup>14–23</sup> Jaeger et al.<sup>14</sup> investigated the infrared photodissociation spectroscopy of cationic TMBz and  $\text{TMBz}_2$  complexes in the gas-phase spectra and characterized vibrational bands in the 600–1700  $\text{cm}^{-1}$  region with DFT computations; systematic shifts of the bands of the Bz molecule caused by the metal bonding were observed. The neutral TMBz and  $\text{TMBz}_2$  complexes were investigated with infrared spectroscopy and DFT computations, and the ground-state structures and vibrational frequency were well-determined.<sup>15–17</sup> Nagaoka et al.<sup>18</sup> extended the soft-landing infrared reflection absorption spectroscopy to the multidecker sandwich  $\text{V}_2\text{Bz}_3$  and characterized the typical bands in the range of the 600–1600  $\text{cm}^{-1}$  region. We explored the size-specific infrared spectra of  $\text{V}_n\text{Bz}_{n+1}$ ,  $n = 1-6$  with DFT computations and provided a possible way to verify the structural transition from achiral  $D_{6h}$  structure to chiral  $D_2$  structure with broadened IR spectra or

with the appearance of new IR modes.<sup>19</sup> On the other hand, Imura et al.<sup>20</sup> determined the electric dipole moment of  $\text{TiBz}$  is  $2.4 \pm 0.3$  D. Rabilloud et al.<sup>21</sup> explored the dipole moment of half-sandwiches TMBz (TM = Sc, Ti, V) and found ScBz has the large dipole moment of  $1.6 \pm 0.3$  D, in contrast to the much smaller moment of  $0.17 \pm 0.3$  D for VBz. Rabilloud<sup>22</sup> also made complete active space self-consistent field (SCF) and multireference configuration interaction calculations on the TMBz (TM = Sc, Ti, V) sandwiches and found the dipole moment is 0.90, 0.60, and 0.47 D, respectively. Rayane et al.<sup>23</sup> performed the electric dipole moment measurements and DFT calculations on the smallest full sandwiches  $\text{TMBz}_2$  (TM = Sc, Ti, V, Nb, Ta, Zr, Ni, Co) and obtained  $0.7 \pm 0.3$  and  $1.3 \pm 0.3$  D for  $\text{CoBz}_2$  and  $\text{NiBz}_2$  and nearly zero for other complexes. Whereas the dipole moments reflect the charge distributions within the  $\text{TM}_n\text{Bz}_m$  complexes, the linear polarizabilities measure their response against an external field, both being widely used in understanding the structural and electronic properties of the cluster systems.<sup>24–26</sup> However, there still lacks any experimental and theoretical reports on the linear polarizability of transition metal–Bz complexes. The goal of this article is to study the dipole moment and linear polarizabilities of the  $\text{Co}_n\text{Bz}_m$  clusters of  $m = n, n + 1, m, n = 1-4$  within the framework of an all-electron gradient-corrected DFT. In our previous study,<sup>13</sup> we have revealed that the two types of structures, sandwich and rice-ball, are energetically competitive in  $\text{Co}_n\text{Bz}_m$  clusters. In this study, we explored the polarizabilities of these clusters using a DFT-based finite field approach. Both the geometric effect and the electronic effect on polarizabilities are addressed, and a close relationship between cluster volume and polarizability is observed, which is then used to understand the polarizability variations in the  $\text{Co}_n\text{Bz}_m$  clusters.

## II. Computational Methodology

The equilibrium geometries were taken from our previous work in which Becke’s functional with the correlation functional of Lee, Yang, and Parr (BLYP)<sup>27,28</sup> as well as a double-

\* Corresponding authors. E-mail: jlwang@seu.edu.cn (J.W.); myang@scu.edu.cn (M.Y.).

† Southeast University.

‡ Sichuan University.

numerical basis set including d- or p-polarization functions (DNP) for Co, C, and H atoms were exploited, implemented within the DMol3 package.<sup>29</sup> The methodology justification was assessed for the Co atom,  $\text{Co}_2$  dimer, and  $\text{C}_6\text{H}_6$  molecule, and the details can be found in ref 13.

The static electric dipole moment and polarizability components were calculated using the combination of BLYP/DNP and Kurtz's finite field (FF) approach.<sup>30</sup> The DNP basis set has been used in studying the polarizability and second-order hyperpolarizability of  $\text{C}_{50}\text{Cl}_{10}$  clusters and produces comparable results with other theoretical studies.<sup>31</sup> The dipole moment  $\mu_i$  and polarizability component  $\alpha_{ij}$  are evaluated, respectively, as

$$\mu_i = -\left(\frac{\partial E}{\partial F_i}\right) \quad (1)$$

and

$$\alpha_{ij} = -\left(\frac{\partial^2 E}{\partial F_i \partial F_j}\right) \quad (i, j = x, y, z) \quad (2)$$

where  $E$  is the total energy of the complex and  $F_i$  ( $i = x, y, z$ ) are components of the applied field in different directions. One of the problems in the finite field method is the choice of field strength. Sim et al.<sup>32</sup> found that stable linear and nonlinear polarizabilities can be obtained when  $F_i$  are in the range of 0.001–0.005 au. In this work, the external field strength  $F_i$  was set to 0.005 au. A tight SCF convergence criterion was adopted to ensure the precision of the computed polarizability. We have justified our computational strategy by computing the polarizabilities of a single Co atom and benzene molecule, which are 9.10 and 11.73  $\text{\AA}^3$ , respectively, in reasonable agreement with the measured values of 9.99<sup>33</sup> and 10.54  $\text{\AA}^3$ <sup>34</sup> and the previously computed value of 10.09  $\text{\AA}^3$  at the CCSD/aug-cc-pVQZ level<sup>35</sup> for benzene. Neither experimental nor theoretical polarizability for the Co atom is available to our knowledge. We have performed MP2 and CCSD(T) calculations with the LANL2DZ basis set implemented in Gaussian03<sup>36</sup> on the Co atom and obtained the polarizabilities of 10.86 and 10.75  $\text{\AA}^3$ , respectively, which are close to our BLYP/DNP result. As polarizability calculations become computationally demanding for large systems, this combination reaches a good compromise between accuracy and computational cost and may give a reasonable description of the static electric dipole and linear polarizability of the Co–Bz complexes.

### III. Results and Discussion

In our previous work,<sup>13</sup> we performed an all-electron gradient-corrected DFT study on the geometrical and electronic properties of  $\text{Co}_n\text{Bz}_m$ , ( $n, m = 1-4, m = n, n + 1$ ) clusters, and two families of structures, sandwich and rice-ball, were identified and are energetically competitive. For the sizes smaller than (2, 3), sandwich conformations are preferred, whereas the rice-ball structures are more favorable for  $n \geq 3$ . For the case of  $\text{Co}_2\text{Bz}_3$ , the sandwich structure is most stable, and the rice-ball structure is only 0.117 eV higher in energy with a comparable highest occupied molecular orbital–lowest unoccupied molecular orbital (HOMO–LUMO) gap and ionization energy, indicating the coexistence of both structures as suggested from chemical reaction experiments.<sup>3</sup> The most stable structures and their metastable isomers of the Co–Bz complexes are displayed in Figure 1.

On the basis of the optimized structures of  $\text{Co}_n\text{Bz}_m$ , ( $n, m = 1-4, m = n, n + 1$ ) clusters displayed in Figure 1, we calculated their dipole moments and static polarizabilities with the finite

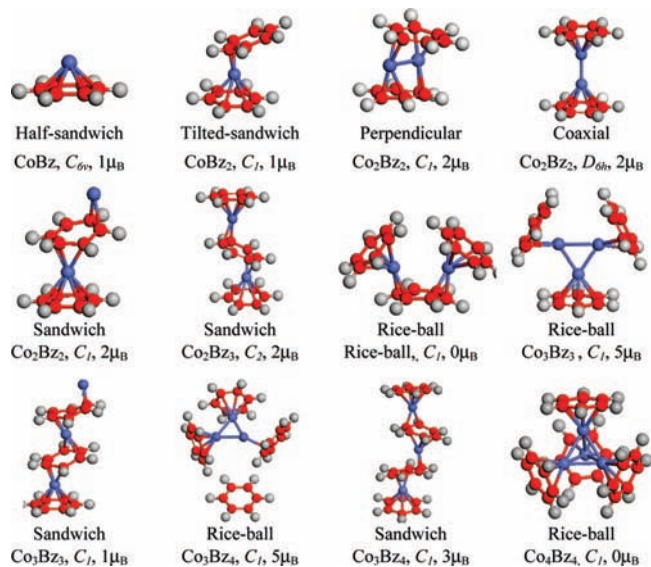


**Figure 1.** Most stable structures and low-lying isomers of  $\text{Co}_n\text{Bz}_m$  ( $n, m = 1-4, m = n, n + 1$ ) complexes.

field approach. The computed dipole moment, mean and anisotropic polarizability, together with the relative energies, HOMO–LUMO gaps, ionization energies, and volumes of the clusters are presented in Table 1. The dipole moments are all relatively large (around 0.5–1.65 D) except the coaxial  $\text{Co}_2\text{Bz}_2$  ( $\bullet \bullet$ ) and the rice-ball  $\text{Co}_4\text{Bz}_4$ , indicating that most of these clusters possess asymmetric structures. The nearly zero dipole moments in the coaxial  $\text{Co}_2\text{Bz}_2$  and rice-ball  $\text{Co}_4\text{Bz}_4$  mainly stem from their symmetrically geometric feature. The former has highly symmetric  $D_{6h}$  structure with the Co–Co bond collinear with the  $C_6$  axis of the benzene ring, and the latter is roughly in  $T_d$  symmetry. Thus, their charge distributes symmetrically around the geometric centers (principal axis) of the clusters, and this results in very small values in dipole moment. However, we should point out that the computed dipole of 1.61 D is quite a bit larger than the measured value of  $0.7 \pm 0.3$  D<sup>23</sup> along the principal inertial axis of the  $\text{CoBz}_2$  complex, although it is in good agreement with the earlier theoretical computation by the same group (1.58 D).<sup>23</sup> This indicates that some uncertainty still remains either in theory or experiment for  $\text{CoBz}_2$ .

To illustrate the size dependence of the polarizability, we plot the total and average polarizabilities per unit, defined as  $\alpha/(n + m)$ , of the lowest energy structure of the complexes in Figure 2. The total polarizability increases monotonically with increasing cluster size from 11.47  $\text{\AA}^3$  of  $\text{CoBz}$  to 56.67  $\text{\AA}^3$  of  $\text{Co}_4\text{Bz}_4$ , while the increase of adding one more benzene is more significant than that of adding one more Co atom. One may also note that the increase of the total polarizability becomes slower for larger size, which is highlighted in Figure 2a. The average polarizability per unit shows “odd–even” oscillation with larger values at ( $n, n + 1$ ) than their neighboring ( $n, n$ ), and the magnitude tends to increase from (1, 1) to (2, 3) but decreases from (2, 3) to (4, 4).

To address the shape dependence, we investigated the polarizability of the sandwich and the rice-ball structures as a function of cluster size separately. As displayed in Figure 3, the polarizabilities increase linearly with cluster size for both kinds of structures while the sandwiches have larger values (about 5.5–15.2  $\text{\AA}^3$ ) than their rice-ball isomers, indicating that the geometric effect plays an important role in determining the polarizability of the complexes.

**TABLE 1: Structure/Point Group Symmetry (PGS), Spin Multiplicity ( $M$ ), Relative Energy ( $\Delta E$ ), Spin-Allowed HOMO–LUMO Gap ( $\Delta$ ), Vertical Ionization Energy (VIP), Volume, Dipole Moment ( $\mu$ ), Polarizability ( $\alpha$ ), and Polarizability Anisotropy ( $\Delta\alpha$ ) of the Co–Bz Complexes**

system	structure/PGS	$M$	$\Delta E$ (eV)	$\Delta$ (eV)	VIP (eV)	vol (cm <sup>3</sup> /mol)	$\mu$ (D)	$\alpha$ (Å <sup>3</sup> )	$\Delta\alpha$ (Å <sup>3</sup> )
CoBz	half-sand/ $C_{6v}$	2	0.000	0.841	5.468	79.51	1.435	11.47	4.45
CoBz <sub>2</sub>	sand/ $C_1$	2	0.000	1.148	5.614	135.30	1.650	23.42	7.15
Co <sub>2</sub> Bz <sub>2</sub>	per/ $C_1$	3	0.000	0.943	5.353	161.36	1.034	26.80	8.53
	col/ $D_{6h}$	3	1.041	0.489	5.032	147.70	0.000	34.82	35.32
	sand/ $C_1$	3	1.209	0.542	5.525	155.05	0.874	35.60	36.23
Co <sub>2</sub> Bz <sub>3</sub>	sand/ $C_2$	3	0.000	1.256	5.107	224.41	0.504	43.32	36.38
	rice/ $C_1$	1	0.117	1.201	4.980	235.41	1.559	37.72	15.06
Co <sub>3</sub> Bz <sub>3</sub>	rice/ $C_1$	6	0.000	1.052	4.855	252.60	1.271	46.82	20.87
	sand/ $C_1$	2	1.721	0.960	4.870	232.48	1.170	55.77	72.32
Co <sub>3</sub> Bz <sub>4</sub>	rice/ $C_1$	6	0.000	1.018	4.800	300.07	1.374	54.77	9.24
	sand/ $C_1$	4	0.567	0.819	4.566	281.55	1.623	69.95	86.43
Co <sub>4</sub> Bz <sub>4</sub>	rice/ $C_1$	1	0.000	1.105	4.415	313.75	0.043	56.67	0.09

To further characterize the dependence of polarizability on the shape of the clusters, we explored the anisotropy of the polarizability  $\Delta\alpha$ , defined as<sup>37</sup>

$$\Delta\alpha = \left(\frac{1}{2}\right)^{1/2} [(\alpha_{xx} - \alpha_{yy})^2 + (\alpha_{yy} - \alpha_{zz})^2 + (\alpha_{zz} - \alpha_{xx})^2 + 6(\alpha_{xy}^2 + \alpha_{yz}^2 + \alpha_{zx}^2)]^{1/2} \quad (3)$$

where the off-diagonal components are found to be very small and can be negligible for the Co<sub>*n*</sub>Bz<sub>*m*</sub> complexes.

As one can see from Table 1 and Figure 3, bottom, the sandwich structures have much larger  $\Delta\alpha$  than the rice-ball structures. The  $\Delta\alpha$  of the sandwich structure is relatively small at the smallest sizes of (1, 1) and (1, 2) and increases markedly as cluster size increases. This is because these two clusters can be viewed as the roughly spherical structure for small sizes, and therefore their polarizabilities do not exhibit distinct anisotropy. However, as the cluster size increases, the anisotropy of the polarizability becomes significant, corresponding to the

prolate motif of the structures. It is interesting to note that the sandwich structures show two smooth increasing steps at (1, 1) to (1, 2) and (2, 2) to (2, 3). The additional Bz molecule in the sandwiches lies in the plane perpendicular to the metal–ligand axis and therefore enhances the polarizability contribution not only along the axis but also along the other two directions in the Bz plane, leading to very small increase of  $\Delta\alpha$ . However, the anisotropies of the rice-ball structures are rather complicated. The  $\Delta\alpha$  increases from (1, 1) to (2, 3), peaks at (3, 3), and decreases afterward. This can be understood in terms of their structural variation with size. The small  $\Delta\alpha$  corresponds to the spherical rice-ball structures. The shape of the cluster is altered remarkably for small clusters when adding one Co atom or Bz molecule. However, after it forms the spherical rice-ball at (3, 3), the addition of another Co atom or Bz molecule does not change the shape of the cluster dramatically. The spherical shape remains but is in larger size (volume). Moreover, the large rice-balls, (3, 3) and (3, 4), are more spherical in geometry and have rather smaller  $\Delta\alpha$  in contrast. Therefore, the largest  $\Delta\alpha$  is obtained at (3, 3). The significantly different anisotropy behavior again confirms the polarizability is closely correlated with the shape of the complex.

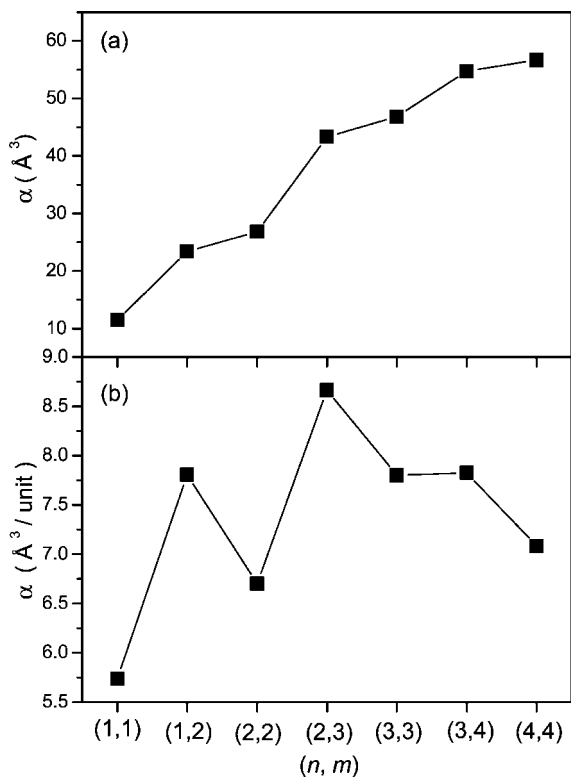


**Figure 2.** Polarizability of the lowest energy structures of Co<sub>*n*</sub>Bz<sub>*m*</sub>,  $m = 1-4$ ,  $m = n$ ,  $n + 1$ : (a) total  $\alpha$ ; (b) average  $\alpha$  per unit.

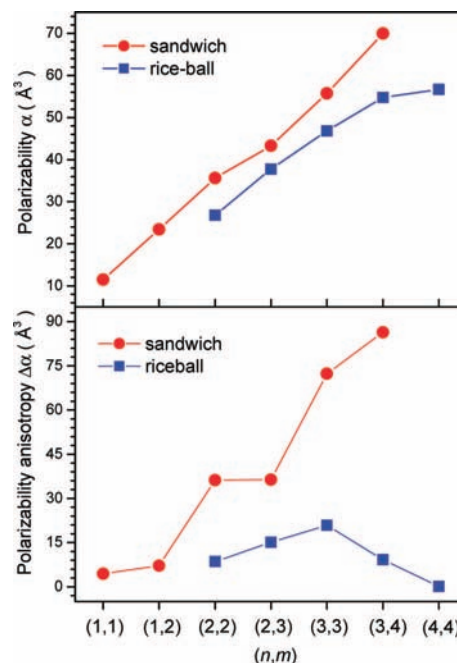


**Figure 3.** (Top) Polarizability and (bottom) polarizability anisotropy of the sandwich and rice-ball structures of Co<sub>*n*</sub>Bz<sub>*m*</sub>,  $m = 1-4$ ,  $m = n$ ,  $n + 1$ .

Polarizability measures the overall electronic charge redistribution in the presence of an external field and is usually favored by weak binding of the electron to the cluster and/or a large volume of electron delocalization. The binding strength can be estimated with either the HOMO–LUMO gap or vertical ionization energy of the cluster. In fact, the polarizability of pull–push systems can be estimated qualitatively with a simple two-state model in which a small HOMO–LUMO gap tends to generate large polarizability.<sup>38</sup> Such correlation is observed in some of the  $\text{Co}_n\text{Bz}_m$  clusters. For open-shell electronic configurations, the gaps between the HOMO and the LUMO of the majority and minority manifolds that correspond to spin-allowed electron transitions were considered, and only the smaller one is presented in Table 1. For example, the HOMO–LUMO gap of the sandwich structure of  $\text{Co}_3\text{Bz}_3$  is 0.960 eV, corresponding to the polarizability as high as 55.77 Å<sup>3</sup>, whereas the gap of its rice-ball isomer is 1.052 eV and the polarizability is only 46.82 Å<sup>3</sup>. This correlation, however, does not hold for other complexes. For example, both the HOMO–LUMO gap and the polarizability of the (2, 2) coaxial structure are smaller than those of its sandwich isomer. The two (2, 3) isomers have comparable HOMO–LUMO gaps but much different polarizabilities. In perturbation theory, polarizability is expressed as a sum of contributions from all excited states.<sup>39</sup> A clear correlation between polarizability and the HOMO–LUMO gap may hold if the dominant excited states are mostly described by the transition from HOMO to LUMO, like the case of one-dimensional push–pull systems. Our results indicate that the electron excitations in the  $\text{Co}_n\text{Bz}_m$  complexes are complicated and their HOMO–LUMO transitions are inadequate to describe the polarizability variations well. Contributions from other transitions may also have considerable effect on the polarizabilities.

Ionization energy (IE) is a quantity indicating the capability of the cluster to lose one valence electron. Chandrakumar et al.<sup>40</sup> found that the cube root of polarizability ( $\alpha^{1/3}$ ) is inversely proportional to the ionization energy ( $V_{\text{ion}}^{-1}$ ) for both the sodium and lithium clusters. This is easy to understand since the higher IE means a stronger binding of the cluster to the valence electron that consequently constrains the distortion of the electron density under an external static electric field and leads to smaller static polarizability. To explore the correlation between polarizability and IE, the variation of  $\alpha^{1/3}$  as a function of  $V_{\text{ion}}^{-1}$  is displayed in Figure 4 for both the sandwich and rice-ball structures. Linear trends are clearly observed separately for the rice-ball and sandwich structures except the  $\text{CoBz}$  half-sandwich.

To give a clear picture of the electron delocalization/localization, the HOMO and LUMO isodensity surfaces of the sandwich and rice-ball structures of  $\text{Co}_2\text{Bz}_3$  and  $\text{Co}_3\text{Bz}_3$  are presented in Figure 5. It clearly shows that the HOMO density is mostly localized on metal Co atoms for both the sandwich and rice-ball structures. However, the LUMO density is shared by Co atoms and Bz molecules in the rice-ball structures and is mainly localized in Co atoms in the sandwich structures. From HOMO to LUMO, the density varies in different ways for these two-family structures. The electrons flow to surrounding benzenes in the rice-balls but to other Co atom(s) through the benzene(s) in the sandwiches, indicating that the electrons in the sandwiches under an external electric field may transfer in a wider range and lead to a larger change in dipole moment and in consequence larger polarizabilities.

The shape-dependent polarizability can be further understood in terms of electron delocalization volume, which is computed by integrating all points in the space with electron density greater

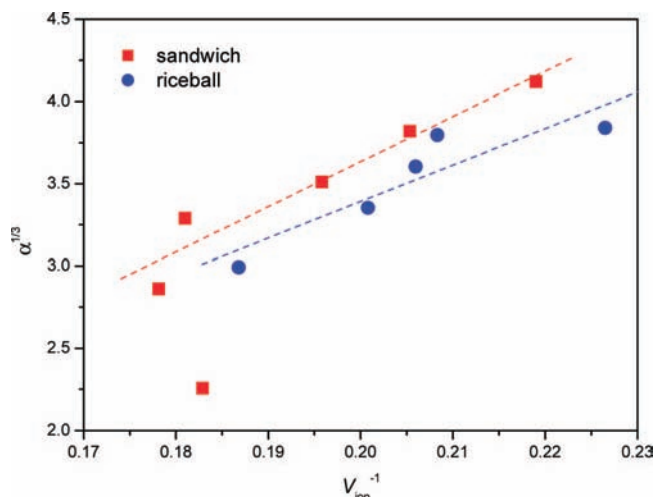


**Figure 4.** Relationship between the polarizability ( $\alpha^{1/3}$ ) and the ionization energy ( $V_{\text{ion}}^{-1}$ ) of the lowest energy sandwich and the rice-ball structures for  $\text{Co}_n\text{Bz}_m$ .

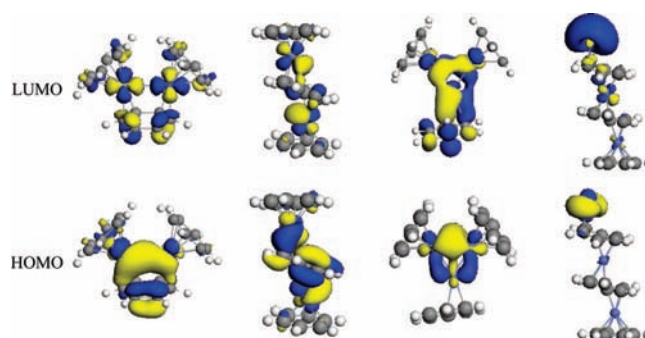


**Figure 5.** Isodensity surfaces of the HOMOs and LUMOs of the rice-ball and sandwich structures of  $\text{Co}_2\text{Bz}_3$  and  $\text{Co}_3\text{Bz}_3$ .

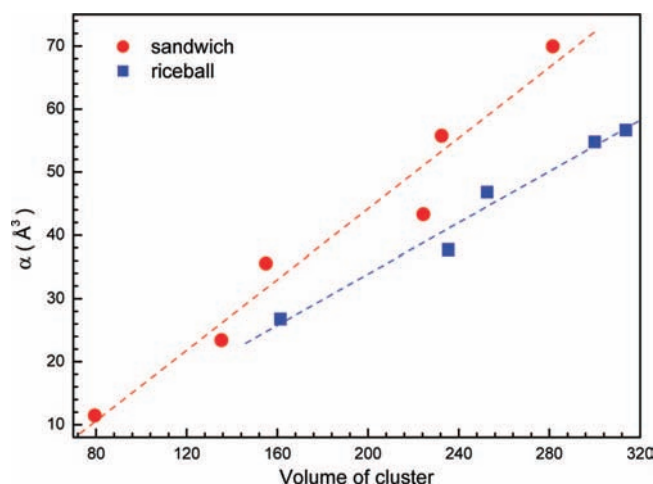


**Figure 6.** Total polarizability of the lowest energy structures of  $\text{Co}_n\text{Bz}_m$ ,  $m = 1-4$ ,  $m = n, n + 1$ , vs cluster volume.

than 0.001 au, as recommended by Bader.<sup>41</sup> Figure 6 shows a close correlation between the polarizability and the cluster volume. The polarizabilities of both the sandwich and the rice-ball structures increase monotonically with their volumes, respectively. The sandwich structure has larger volume than the corresponding rice-ball isomer because there is less volume shared by multiple atoms in the former. The nearly linear increase of polarizability with volume shown in Figure 6 indicates that the volume is one of the crucial factors in determining the polarizabilities of the clusters. Interestingly, both

the sandwich and rice-ball structures exhibit a linear dependence in polarizability, but in different patterns that are determined by their electronic properties, as discussed above. Therefore, both the geometric effect and electronic effect coplay in determining the polarizability of the  $\text{Co}_m\text{Bz}_n$  complexes.

#### IV. Conclusion

In summary, we report a study on the dipole moments and static polarizabilities of  $\text{Co}_n\text{Bz}_m$ , ( $n, m = 1-4, m = n, n + 1$ ) clusters by a combination of an all-electron gradient-corrected DFT and finite field approach. The dipole moments are relatively large except for the  $\text{Co}_2\text{Bz}_2$   $D_{6h}$  coaxial structure and  $\text{Co}_4\text{Bz}_4$  rice-ball structure, which correspond to their asymmetric structures. The total polarizability of the most stable structure of the complexes increase rapidly with cluster size, whereas the average polarizability shows "odd-even" alternation and larger values at ( $n, n + 1$ ) than ( $n, n$ ). The sandwich structures have systematically larger polarizability and anisotropy than their rice-ball isomers, indicating a close correlation between the polarizability and the cluster shape. Although no simple correlation is found between the HOMO-LUMO gap and the polarizability, a linear dependence of polarizability on cluster volume is identified for the sandwich and rice-ball structures, respectively. The inverse relationship is also identified between the polarizability and the IE. Both the geometric and electronic effects play crucial roles in the determination of the polarizabilities of the  $\text{Co}_n\text{Bz}_m$  clusters. The markedly different polarizabilities in sandwich and rice-ball structures suggest a possible way to distinguish them by inspecting their polarizabilities theoretically or experimentally.

**Acknowledgment.** The work is supported by the National Nature Science Foundation of China (No. 10604013), the Program for New Century Excellent Talents in the University of China (NCET-06-0470), the project sponsored by SRF for ROCS, SEM, the Qinglan Project in the University of Jiangsu Province, and the Teaching and Research Foundation for the Outstanding Young Faculty of Southeast University. The authors thank the computational resource at Department of Physics, Southeast University.

#### References and Notes

- Long, N. J. *Metalloenes*; Blackwell Science: Oxford, 1998.
- Nakajima, A.; Kaya, K. *J. Phys. Chem. A* **2000**, *104*, 176.
- Kurikawa, T.; Hirano, M.; Takeda, H.; Yagi, K.; Hoshino, K.; Nakajima, A.; Kaya, K. *J. Phys. Chem.* **1995**, *99*, 16248.
- Weis, P.; Kemper, P. R.; Bowers, M. T. *J. Phys. Chem. A* **1997**, *101*, 8207.
- Gerhards, M.; Thomas, O. C.; Nilles, J. M.; Zheng, W. J.; Bowen, K. H., Jr. *J. Chem. Phys.* **2002**, *116*, 23.
- Knickerbein, M. B. *J. Chem. Phys.* **2006**, *125*, 044308.
- Miyajima, K.; Yabushita, S.; Knickerbein, M. B.; Nakajima, A. *J. Am. Chem. Soc.* **2007**, *129*, 8473.
- Kandalam, A. K.; Rao, B. K.; Jena, P.; Pandey, R. *J. Chem. Phys.* **2004**, *120*, 10414.
- Wang, J.; Acioli, P. H.; Jellinek, J. *J. Am. Chem. Soc.* **2005**, *127*, 2812.
- Maslyuk, V. V.; Bagrets, A.; Meded, V.; Arnold, A.; Evers, F.; Brandbyge, M.; Bredow, T.; Mertig, I. *Phys. Rev. Lett.* **2006**, *97*, 097201.
- Xiang, H. J.; Yang, J. L.; Hou, J. G.; Zhu, Q. S. *J. Am. Chem. Soc.* **2006**, *128*, 2310.
- Kua, J.; Tomlin, K. M. *J. Phys. Chem. A* **2006**, *110*, 11988.
- Zhang, X.; Wang, J. *J. Phys. Chem. A* **2008**, *112*, 296.
- Jaeger, T. D.; Heijnsbergen, D. V.; Klippenstein, S. J.; Helden, G.; Meijer, G.; Duncan, M. A. *J. Am. Chem. Soc.* **2004**, *126*, 10981.
- Judai, K.; Sera, K.; Amatsutsumi, S.; Yagi, K.; Yasuie, T.; Yabushita, S.; Nakajima, A.; Kaya, K. *Chem. Phys. Lett.* **2001**, *334*, 277.
- Lyon, J. T.; Andrews, L. *J. Phys. Chem. A* **2005**, *109*, 431.
- Bechamp, K.; Levesque, M.; Joly, H.; Manceron, L. *J. Phys. Chem. A* **2006**, *110*, 6023.
- Nagaoka, S.; Matsumoto, T.; Ikemoto, K.; Mitsui, M.; Nakajima, A. *J. Am. Chem. Soc.* **2007**, *129*, 1528.
- Wang, J.; Jellinek, J. *J. Phys. Chem. A* **2005**, *109*, 10180.
- Imura, K.; Ohoyama, H.; Kasai, T. *Chem. Phys. Lett.* **2003**, *369*, 55.
- Rabilloud, F.; Rayane, D.; Allouche, A. R.; Antoine, R.; Aubert-Frecon, M.; Broyer, M.; Compagnon, I.; Dugourd, Ph. *J. Phys. Chem. A* **2003**, *107*, 11347.
- Rabilloud, F. *J. Chem. Phys.* **2005**, *122*, 134303.
- Rayane, D.; Allouche, A. R.; Antoine, R.; Broyer, M.; Compagnon, I.; Dugourd, P. *Chem. Phys. Lett.* **2003**, *375*, 506.
- Papadopoulos, M. G.; Reis, H.; Avramopoulos, A.; Erkok, S.; Amirouche, L. *J. Phys. Chem. B* **2005**, *109*, 19922.
- Jackson, K. A.; Yang, M.; Chaudhuri, I.; Frauenheim, T. *Phys. Rev. A* **2005**, *71*, 33205.
- Rosso, A.; Lindblad, A.; Lundwall, M. *J. Chem. Phys.* **2007**, *127*, 24302.
- Becke, A. D. *J. Chem. Phys.* **1988**, *88*, 2547.
- Lee, C.; Yang, W.; Parr, R. G. *Phys. Rev. B* **1988**, *37*, 785.
- DMOL is a density functional theory program distributed by Accelrys, Inc. Delley, B. *J. Chem. Phys.* **1990**, *92*, 508; *J. Chem. Phys.* **2000**, *113*, 7756.
- Kurtz, H. A.; Stewart, J. J. P.; Dieter, K. M. *J. Comput. Chem.* **1990**, *11*, 82.
- Yang, Y.; Wang, F. H.; Zhou, Y. S.; Yuan, L.; Yang, J. *Phys. Rev. A* **2005**, *71*, 013202.
- Sim, F.; Chin, S.; Dupuis, M.; Rice, J. E. *J. Phys. Chem.* **1993**, *97*, 1158.
- Hasanein, A. A. *Adv. Chem. Phys.* **1993**, *85*, 415.
- Ritchie, G. L. D.; Watson, J. N. *Chem. Phys. Lett.* **2000**, *322*, 143.
- Hammond, J. R.; Kowalski, K.; deJong, W. A. *J. Chem. Phys.* **2007**, *127*, 144105.
- Frisch, M. J.; Trucks, G. W.; Schlegel, H. B.; Scuseria, G. E.; Robb, M. A.; Cheeseman, J. R.; Montgomery, J. A., Jr.; Vreven, T.; Kudin, K. N.; Burant, J. C.; Millam, J. M.; Iyengar, S. S.; Tomasi, J.; Barone, V.; Mennucci, B.; Cossi, M.; Scalmani, G.; Rega, N.; Petersson, G. A.; Nakatsuji, H.; Hada, M.; Ehara, M.; Toyota, K.; Fukuda, R.; Hasegawa, J.; Ishida, M.; Nakajima, T.; Honda, Y.; Kitao, O.; Nakai, H.; Klene, M.; Li, X.; Knox, J. E.; Hratchian, H. P.; Cross, J. B.; Adamo, C.; Jaramillo, J.; Gomperts, R.; Stratmann, R. E.; Yazyev, O.; Austin, A. J.; Cammi, R.; Pomelli, C.; Ochterski, J. W.; Ayala, P. Y.; Morokuma, K.; Voth, G. A.; Salvador, P.; Dannenberg, J. J.; Zakrzewski, V. G.; Dapprich, S.; Daniels, A. D.; Strain, M. C.; Farkas, O.; Malick, D. K.; Rabuck, A. D.; Raghavachari, K.; Foresman, J. B.; Ortiz, J. V.; Cui, Q.; Baboul, A. G.; Clifford, S.; Cioslowski, J.; Stefanov, B. B.; Liu, G.; Liashenko, A.; Piskorz, P.; Komaromi, I.; Martin, R. L.; Fox, D. J.; Keith, T.; Al-Laham, M. A.; Peng, C. Y.; Nanayakkara, A.; Challacombe, M.; Gill, P. M. W.; Johnson, B.; Chen, W.; Wong, M. W.; Gonzalez, C.; Pople, J. *Gaussian 03*; Gaussian, Inc.: Pittsburgh, PA, 2003.
- Karamanis, P.; Pouchan, C.; Maroulis, G. *Phys. Rev. A* **2008**, *77*, 013201.
- Vasiliev, I.; Ogut, S.; Chelikowsky, J. R. *Phys. Rev. Lett.* **1997**, *78*, 4805.
- Orr, B. J.; Ward, J. F. *Mol. Phys.* **1971**, *20*, 513.
- Chandrakumar, K. R. S.; Ghanty, T. K.; Ghosh, S. K. *J. Phys. Chem. A* **2004**, *108*, 6661.
- Bader, R. F. W. *Atoms in Molecules: A Quantum Theory*; Oxford University Press: New York, 1990.